BIOMOLECULES & THERAPEUTICS

Original Article
Biomol Ther 29(6), 615-629 (2021)

Neuroprotective Effect of Astersaponin I against Parkinson's Disease through Autophagy Induction

Lijun Zhang[1,2,3], Jeoung Yun Park[1], Dong Zhao[1,2], Hak Cheol Kwon[4] and Hyun Ok Yang[1,2,5,*]

[1]Natural Product Research Center, Korea Institute of Science and Technology, Gangneung 25451,
[2]Division of Bio-Medical Science and Technology, KIST School, Korea University of Science and Technology, Seoul 02792, Republic of Korea
[3]State Key Laboratory for Chemistry and Molecular Engineering of Medical Resources, Guangxi Normal University, Guilin 541004, China
[4]Natural Product Informatics Research Center, Korea Institute of Science and Technology, Gangneung 25451,
[5]Department of Integrative Biological Sciences and Industry, Sejong University, Seoul 05006, Republic of Korea

Abstract

An active compound, triterpene saponin, astersaponin I (AKNS-2) was isolated from *Aster koraiensis* Nakai (AKNS) and the autophagy activation and neuroprotective effect was investigated on *in vitro* and *in vivo* Parkinson's disease (PD) models. The autophagy-regulating effect of AKNS-2 was monitored by analyzing the expression of autophagy-related protein markers in SH-SY5Y cells using Western blot and fluorescent protein quenching assays. The neuroprotection of AKNS-2 was tested by using a 1-methyl-4-phenyl-2,3-dihydropyridium ion (MPP^+)-induced *in vitro* PD model in SH-SY5Y cells and an MPTP-induced *in vivo* PD model in mice. The compound-treated SH-SY5Y cells not only showed enhanced microtubule-associated protein 1A/1B-light chain 3-II (LC3-II) and decreased sequestosome 1 (p62) expression but also showed increased phosphorylated extracellular signal–regulated kinases (p-Erk), phosphorylated AMP-activated protein kinase (p-AMPK) and phosphorylated unc-51-like kinase (p-ULK) and decreased phosphorylated mammalian target of rapamycin (p-mTOR) expression. AKNS-2-activated autophagy could be inhibited by the Erk inhibitor U0126 and by AMPK siRNA. In the MPP^+-induced *in vitro* PD model, AKNS-2 reversed the reduced cell viability and tyrosine hydroxylase (TH) levels and reduced the induced α-synuclein level. In an MPTP-induced *in vivo* PD model, AKNS-2 improved mice behavioral performance, and it restored dopamine synthesis and TH and α-synuclein expression in mouse brain tissues. Consistently, AKNS-2 also modulated the expressions of autophagy related markers in mouse brain tissue. Thus, AKNS-2 upregulates autophagy by activating the Erk/mTOR and AMPK/mTOR pathways. AKNS-2 exerts its neuroprotective effect through autophagy activation and may serve as a potential candidate for PD therapy.

Key Words: Autophagy, Parkinson's disease, Neuroprotection, Tyrosine hydroxylase, Motor symptoms

INTRODUCTION

Parkinson's disease (PD) is the second most common neurodegenerative disease after Alzheimer's disease. The central pathological feature of PD is the loss of dopaminergic neurons in the substantia nigra pars compacta (SNpc). Lewy bodies (LBs) form due to the abnormal accumulation of α-synuclein in the neurons is another neuropathology of PD (Poewe *et al*., 2017). Moreover, abnormal motor symptoms are frequently found in PD patients (Dauer and Przedborski, 2003).

1-Methyl-4-phenyl-1,2,3,6-tetrahydropyridine (MPTP), is a potent neurotoxin that can destroy dopaminergic neurons in the SNpc (Kostrzewa, 2014). In many kinds of animals, MPTP produces severe and irreversible symptoms similar to those in PD. Once MPTP crosses the blood-brain barrier (BBB), it can be converted to the real toxin 1-methyl-4-phenylpyridinium (MPP^+) by monoamine oxidase type B (MAO-B). A portion of MPP^+ enters mitochondria and blocks the mitochondrial electron transport enzyme NADH dehydrogenase, thus inhibits cellular respiration (Ramsay and Singer, 1986; Klaidman *et al*., 1993). Exposure to MPTP also leads to the pathological aggregation of proteins, including ubiquitin and α-synuclein, and the aggregated proteins cannot be metabolized (Conway *et al*., 2000). MPTP is applied and considered the best experi-

Open Access **https://doi.org/10.4062/biomolther.2021.004**

Received Jan 6, 2021 **Revised** May 17, 2021 **Accepted** Jun 7, 2021
Published Online Jul 2, 2021

***Corresponding Author**
E-mail: hoyang@sejong.ac.kr
Tel: +82-2-3408-1959, Fax: +82-2-3408-4336

mental tool to mimic the specific features of PD.

Autophagy is a self-degradative process, and it is important to balance energy sources and adapt to nutrient stress. Autophagy is a crucial survival mechanism and plays a key role in treating various diseases, including neurodegeneration diseases (Glick *et al*., 2010), it can be regulated through a complicated signaling pathway. mTOR complex 1 (mTORC1) reflects cellular nutritional status and links nutrient signals to autophagy regulation (Kim *et al*., 2011). The inhibition of mTORC1 by rapamycin induces autophagy in the presence of nutrients, which demonstrates that TOR is an autophagy inhibitor (Noda and Ohsumi, 1998). AMP-activated protein kinase (AMPK) plays a role in cellular energy homeostasis. AMPK can be activated by low energy levels through the regulation of the upstream kinase LKB1, thereby activating the TSC1/2 complex. The activation of TSC1/2 leads to the inhibition of mTOR activity through inactivating the TOR activator Rheb (He and Klionsky, 2009). AMPK can directly activate ULK1 by upregulating phosphorylation, while it also regulates ULK1 activity through mediating the activity of TSC2 and mTOR1 (Inoki *et al*., 2003; Egan *et al*., 2011). Autophagy can also be up-regulated under nutrient starvation through Erk1/2 activation, Erk1/2 activates autophagy through mTORC1 inhibition via binding to and activating TSC, the depletion of Erk can partially inhibit autophagy (Pattingre *et al*., 2003; Wang *et al*., 2009). Numerous studies indicate that the age-related decline in autophagy disturbs neuronal homeostasis, thus leading to the deposition of toxic components in the cytoplasm and subsequently the progression of neurodegenerative disorders such as PD. Postmortem examinations of brains from PD patients show the distinct accumulation of autophagosomes and loss of lysosomal markers in dopaminergic neurons (Chu *et al*., 2009; Dehay *et al*., 2010).

Aster koraiensis Nakai (AKNS), is commonly distributed in the southern and central parts of the Korean peninsula and Jeju Island (Prabakaran *et al*., 2017). AKNS is used in traditional Korean medicine for treating diseases such as diabetes, chronic bronchitis, pertussis, and pneumonia (Hyun *et al*., 2018; Kim *et al*., 2018). Recently, research by our team reported that a compound, triterpene saponin, astersaponin I (AKNS-2) was isolated from AKNS (Kwon *et al*., 2019), the present research tried to study the effect AKNS-2 on autophagy induction and elucidate the underlying pathways, eventually explore its protective effect on PD.

MATERIALS AND METHODS

Isolation of active compound AKNS-2

The process of *Aster koraiensis* extraction and compound isolation is described in another published research (Kwon *et al*., 2019). Briefly the plant was ground by a pulverizer, and then was extracted with 95 % EtOH solution. Next, the powdered product (named AKNS extract) was extracted by using *n*-hexane, EtOAc and *n*-BuOH, respectively. Subsequently, *n*-BuOH fraction was isolated using a reversed phase HPLC (YMC-Triart C18 column). Finally the mixture of target compounds was separated by Sephadex® LH-20 (GE Healthcare, Chicago, IL, USA). One of the active compounds was purified and the structure was identified as 3-*O*-β-D-xylopyranosyl-(1→3)-β-D-glucopyranosylpolygalacic acid 28-*O*-α-L-rhamnopyranosyl-(1→3)-β-D-xylopyranosyl-(1→4)-[β-D-xylopyranosyl-(1→3)]-α-L-rhamnopyranosyl-(1→2)-α-L-arabinopyranosyl ester, which termed astersaponin I (AKNS-2), using NMR (500 MHz) (showed as Fig. 1).

Materials

Dulbecco's modified Eagle's medium (DMEM), fetal bovine serum (FBS), 100 units/mL penicillin and 100 mg/mL streptomycin are purchased from Gibco (Thermo Fisher Scientific-Waltham, MA, USA). 1-Methyl-4-pheynl-1,2,3,6-tetrahydropyridine (MPTP) hydrochloride, 1-Methyl-4-phenylpyridinium (MPP^+) iodide, 3-methyladenine (3-MA) and ropinirole were purchased from Sigma Chemical Co (St. Louis, MO, USA). Wortmannin (Wort) and bafilomycin A1 (Baf) are from Abcam (MA, USA). Anti-glyceraldehyde-3-phosphate dehydrogenase (GAPDH), anti-AMPK, anti-phosphorylated AMPK (p-AMPK), anti-ULK, anti-phosphorylated ULK555 (p-ULK555), anti-Erk, anti-phosphorylated Erk (p-Erk), anti-mTOR, anti- phosphorylated mTOR (p-mTOR), anti-LC3B, anti-tyrosine hydroxylase (TH), anti-α-synuclein primary antibodies sourced from rabbit, anti-rabbit horseradish peroxidase-conjugated IgG secondary antibody, the Erk inhibitor U0126, the AMPK siRNA, AMPK siRNA control were purchased from Cell Signaling Technology (Boston, MA, USA). An autophagy Tandem Sensor RFP-GFP-LC3B kit was from Thermo Fisher Scientific. MTT assay kit Z-Cytox was from DAEILLAB Co, Ltd (Seoul, Korea). Dopamine ELISA kit was from Abnova (Taipei City, Taiwan) and the MAO-B assay kit was supplied by Promega (Woods Hollow Road Madison, WI, USA). All other chemicals were of the highest

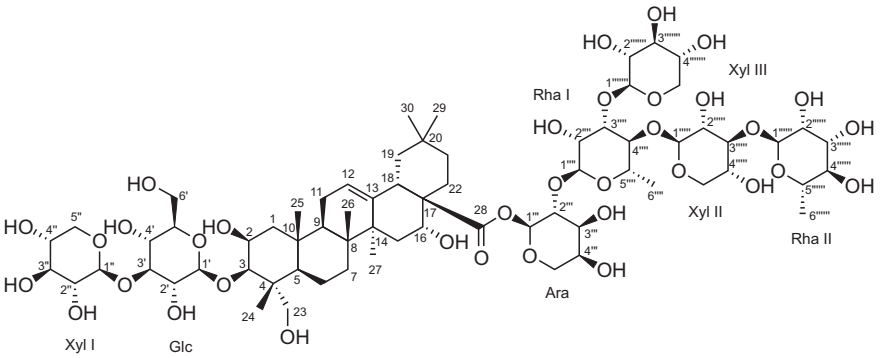

AKNS-2

Fig. 1. Chemical structure of the active compound AKNS-2.

grade and were found from commercial resources.

Cell culture

Human neuroblastoma cells of SH-SY5Y were supplied by the company of American Type Culture Collection (Manassas, VA, USA), and were cultured in DMEM supplemented with 10% heat-inactivated FBS and 1% penicillin/streptomycin. SH-SY5Y cells were incubated under condition of 37°C in humidified atmosphere with 5% CO_2. First cells were seeded on 6-well plate at a density of 80×10^4 cells/well in 2 mL medium, after 24 h were treated with samples AKNS-2 at the desired concentrations. Under the conditions of 3-MA, Wort, Baf or U0126 presence, cells were treated with these reagents 30 min prior to sample treatment. For AMPK siRNA transfected SH-SY5Y cells, AKNS-2 should be administered 36 h after siRNA transfection. When MPP^+ treatment was needed, cells should be treated with MPP^+ 1 h after sample treatment. Twenty-four h after sample treatment, SH-SY5Y cells were harvested and used for further analysis.

MTT assay for measurement of cell viability

Cell viability was detected by using a MTT assay kit Z-Cytox (DAEILLAM Co, Ltd, Seoul, Korea). Briefly, SH-SY5Y cells were seeded on a 96-well plate at a density of 2×10^4 cells/well in 100 μL medium. Twenty-four h later, to determinate the cytotoxicity of AKNS-2 and MPP^+, SH-SY5Y cells were treated with AKNS-2 and/or MPP+ at desired concentrations. After 24 h, 10 μL of MTT reagent was added to each cell containing well of 96-well plate. The absorbance at 450 nm was measured using a microplate spectrophotometer (BioTek, VT, USA). In order to verify the protective effect of AKNS-2 against MPP^+ induced cytotoxicity, we treated cells with 2 mM MPP^+ 1 h after the AKNS-2 treatment. The next day, the absorbance was measured 1 h after addition of MTT reagent. To elucidate if AKNS-2 exerts its protective effect on MPP^+-induced cytotoxicity through autophagy induction, we treated SH-SY5Y cells with U0126 or AMPK siRNA, followed by AKNS-2 (5 and 10 μM) addition 30 min or 36 h later, respectively, 1 h after AKNS treatments, cells were added 2 mM MPP^+.

Measurement of RFP-GFP-LC3 by fluorescence microscope

SH-SY5Y cells were cultured on glass coverslips in 24-well plates at a density of 8×10^4/well. The transfection process were conducted according to the instruction of the Autophagy Tandem Sensors RFP-GFP-LC3B kit (Invitrogen, Carlsbad, CA, USA). After cultivation for 24 h, cells were treated with LC3B reagent. The transfected cells were incubated for 24 h, then 50 nM Wort or 100 nM Baf was administered followed by the addition of AKNS-2 (10 μM). The cells were further fixed with 4% paraformaldehyde and then permeabilized with 0.1% Triton X100. Nuclei were stained with 4,6-diamidino-2-phenylindole (DAPI, 25 μg/mL). Fluorescence signals were detected using a confocal microscope (Leica, Solms, Germany).

Preparation of cell lysates

Twenty-four h after drug treatment, medium in the wells of 6-well plate was discarded and the cells were gently rinsed one time using cold saline. Next, 1 mL cold saline was added to each well, cells adhered to the bottom were suspended by scouring the bottom with a 1 mL pippet. The suspension liquids were collected in 1.5 mL tubes and centrifuged at 13000xg, 4°C for 5 min. After supernatants removal, cell pellets were added 50 μL of RIPA lysis buffer from Cell Signaling Technology containing protease inhibitor cocktail (Roche, Mannheim, Germany). After shaking at 4°C for 30 min, obtained cell samples were centrifuged at 13000xg, 4°C for 20 min. The supernatants were collected and the protein concentrations were measured by Bradford method with a BSA constructed standard curve. Subsequently, supernatants were diluted with loading buffer, and then heated at 99°C for 5 min. The resultant cells samples were used for further Western blot analysis.

Animals

All the animal care and experimental protocols in the present study complied with the guidelines of the Korea Institute of Science and Technology Animal Care Committee (no. 2017-018). All efforts were made to minimize the mice number and relieve their suffering. Forty mice (C57BL/6j, male, 8 weeks old) were ordered from Japan SLC Inc (Shizuoka, Japan). After arrival, four mice were fed in each cage (30×18.5×13 cm) and were supplied with unlimited food and water. All mice were housed under the following constant conditions: lights on from 6:00 to 18:00, temperature of 23 ± 1°C, and humidity of 50 ± 10%. After a habituation period of 7 days, the mice were subjected to a series of experimental operations according to standard protocols.

Animal grouping and sample treatment

Forty mice were divided into 5 groups randomly, with 8 mice in each group. After the habituation period, all mice were orally administered a single dose of drug each day. The mice in group 1 and group 2 were administered saline (p.o.), while the mice in group 3, group 4, and group 5 were administered 5 mg/kg ropinirole (p.o.), 5 mg/kg AKNS-2 (p.o.), and 15 mg/kg AKNS-2 (p.o.), respectively. Here dopamine agonist ropinirole was applied as a positive control. From day 5, the mice in group 1 were intraperitoneally injected with saline 1 h after saline gavage, and the mice in groups 2, 3, 4 and 5 were administered 30 mg/kg MPTP (i.p.) 1 h after the saline, ropinirole, AKNS-2 5 mg/kg and AKNS-2 15 mg/kg gavage, respectively. Each mouse received a single dose of saline/MPTP injection for 8 days. Seven days after the last MPTP injection, all mice were killed by cervical dislocation, and the whole brain, SNpc and striatum (ST) were dissected for further biochemical analysis.

Rotarod test

The rotarod test was conducted following the description (Hu *et al*., 2017a) with minor modifications. Briefly, the test consisted of a pretraining section and a test section. The pretraining section was performed over 4 consecutive days. All mice were placed on the cylinder of the rotarod apparatus with the tail towards the operator, and then the training was started at a constant speed of 16 rpm over a period of 300 s. During this 300 s, the mice that fell to the ground were placed back on the cylinder by the operator. All mice were subjected to a total of 3 trials within a 30-min interval each day before MPTP administration. Beginning on the day after the last behavioral training day, we treated mice with a single dose of 30 mg/kg MPTP for 8 consecutive days 1 h after AKNS-2 (5 and 15 mg/kg) administration. The latency of falling to the ground was recorded for each mouse. For the test section, the performance of all mice on the rotarod was tested following the protocol used during the pretraining section at the 3 time points of 2 h, 24 h and 48 h after the last injection of MPTP. The latency

of each mouse to fall to the ground was recorded. Only mice that remained on the cylinder longer than 60 s in the pretraining section were used in the statistical analysis. The average time of the three trials was calculated to evaluate balance, grip strength and motor coordination.

Pole test

A pole test was conducted following the description in a study (Choi *et al*., 2013) with minor modifications. Briefly, on the day before MPTP administration, a wooden pole (50 cm in length, 1 cm in diameter) with a rough surface was set up in a sound-proof room. Mice were placed on the top of the pole with its head arranged skyward, and the time mice took to turn around and climb down the pole was recorded, up to a maximum of 120 s, by a stopwatch. The same training operation was performed in triplicate within an interval of 30 min. After MPTP injection, the performance of all mice on the pole was tested using the same protocol as in pretraining at the 3 time points of 2 h, 24 h and 48 h after the last MPTP injection. The average time of three trials was analyzed to assess motor function.

Wire hanging test

The wire hanging test was performed according to the study (Zhu *et al*., 2018) with modification. Briefly, a horizontal wire (1.5 mm in diameter, 50 cm in length and 30 cm above the bedding material) was fixed between two poles. Soft bedding was placed underneath the wire. A mouse was handled by the tail and allowed to grasp the middle point of the wire with its forepaws. The timer was started immediately after the proper suspension of the mouse. The time until the mouse fell down from the wire was recorded, up to a maximal duration of 300 s. On the day before MPTP injection, each mouse was subjected to 3 trials, and the average hanging time of 3 trials was analyzed as an index to evaluate balance, muscle function and coordination. At 2 h, 24 h, and 48 h after MPTP injection, we tested mouse performance on the wire hanging task. The average latency of each mouse to fall down to the bedding material was calculated.

Preparation of mouse brain tissue

Seven days after the last injection of MPTP, the SNpc and ST of mice were carefully dissected and stored at –80°C before use. Subsequently, the brain tissues of the SNpc and ST were homogenized in PRO-PREP™ lysis buffer (iNtRON, Gyeonggi, Korea) containing Phosphatase Inhibitor Cocktail Set I (Sigma-Aldrich, MO, USA). After shaking at 4°C for 30 min, the homogenates were centrifuged at 13000×g and 4°C for 20 min, and then the obtained supernatants were collected in a new 1.5 mL tube. The protein concentrations in the supernatants were measured using the Bradford method. A portion of supernatant was mixed with an equal volume of loading buffer and denatured on a 99°C heater for 5 min for Western blot analysis. The remaining supernatants were stored at –80°C for further analysis of MAO-B activity and DA level by ELISA kits (MAO-B activity ELISA kits, Promega, Madison, WI, USA; DA level ELISA kits, Abnova).

Measurement of DA level

DA levels in the ST were measured by a competitive ELISA kit (Abnova) following the manufacturer's instructions. Briefly, the ST was homogenized in 0.01 N HCl in the presence of EDTA and sodium metabisulfite. The homogenate was centrifuged at 13000xg for 5 min. The supernatants were collected and used to measure DA level. After the determination of the protein concentrations in the supernatants, the DA levels in each brain sample were detected in duplicate using an ELISA kit (Abnova). The absorbance at 450 nm was detected by a microreader (BioTek), and the intensity was inversely proportional to the DA level. The DA level is expressed as ng/mg protein.

Determination of MAO-B activity

The MAO-B activity of the ST and SN was determined by a MAO-B assay kit from Promega according to the manufacturer's instructions. The kit applied a homogeneous luminescent method for detecting MAO activity. The assay includes 2 steps. First, the MAO-B substrate was added to MAO-B enzyme-containing material (ST and SN samples) to generate methyl ester luciferin; second, the produced methyl ester luciferin reacted with esterase and luciferase to produce light. The MAO-B activity was directly proportional to the amount of developed light. The luminescent signal was measured using an Infinite M1000 multimode microplate reader (TECAN, Männedorf, Switzerland). MAO-B activity was expressed as relative light units (RLU)/mg protein.

Western blot analysis

The protein markers in the lysates from SH-SHY5Y cells and mouse brain tissues (SNpc and ST) were measured using Western blot analysis. Briefly, after determining the concentration, protein samples (20 μg) were separated by 8%, 10% or 15% sodium dodecyl sulfate-polyacrylamide gel electrophoresis (SDS-PAGE). Then, the separated proteins on the gel were transferred onto a polyvinylidene fluoride (PVDF) buffered saline with 0.1% Tween 20 (TBST) for 5 min, the membrane was blocked with 5% skim milk dissolved in TBST buffer. The membrane was further incubated with monoclonal primary antibodies sourced from rabbits (including anti-GAPDH, anti-AMPK, anti-p-AMPK, anti-ULK, anti-p-ULK555, anti-Erk, anti-p-Erk, anti-mTOR, anti-p-mTOR, anti-LC3B, anti-p62, anti-TH and anti-α-synuclein antibodies). Primary antibodies were diluted to a ratio of 1:1000 in blocking buffer and incubated at 4°C overnight. On the second day, membrane was washed with TBST 3 times (10 min each time) and then incubated in horseradish peroxidase-conjugated goat anti-rabbit IgG secondary antibodies (diluted to a ratio of 1:2000 in blocking buffer) at room temperature. After incubation in secondary antibody for 1 h, the membrane was washed for 30 min. The protein blots on the membrane were developed with an ECL detection kit and visualized using a LAS-4000 mini system (Fujifilm, Tokyo, Japan). Once the protein blot signal saturated, LAS-4000 mini system automatically paints it red color and we stop the detection. In order to accurately quantify the intensity of target protein, only the band showing unsaturated signal should be used for the quantitative analysis (Ghosh *et al*., 2014). The present research chose the unsaturated bands and quantified the intensities of protein with Multi Gauge V3.0 software (Fujifilm).

Statistical analysis

All the data in this study were analyzed using GraphPad Prism 7 software (GraphPad Software, CA, USA) and presented as mean ± SEM. Statistical analysis were carried out using one-way analysis of variance (ANOVA) or Student's *t*-test. A

value of $p<0.05$ was considered statistical significance.

RESULTS

AKNS-2 activated autophagy through the mTOR-dependent signaling pathway

To investigate the autophagy-inducing effects of AKNS-2, SH-SY5Y cells were treated with AKNS-2 at 5, 10, or 20 μM. After treatment for 24 h, the expression levels of autophagy-related protein markers were measured by Western blot analysis. As shown in Fig. 2A, AKNS-2 treatment induced the expression of LC3-II, a key autophagy indicator, in SH-SY5Y cells in a dose-dependent manner. Moreover, AKNS-2 treatment at 10 and 20 μM significantly increased p-Erk expression, while treatment with 5, 10, and 20 μM AKNS-2 led to significant increases in p-AMPK and p-ULK expression. p-mTOR expression was inhibited by 10 and 20 μM AKNS-2. These findings indicate that AKNS-2 may upregulate autophagy by activating the AMPK/mTOR pathway and/or the Erk/mTOR pathway.

3-Methyladenine (3-MA) inhibits the formation of autophagosome (Pattingre *et al*., 2003). To confirm the autophagy activation induced by AKNS-2, we employed 3-MA (5 mM) to disturb the autophagosome accumulation 30 min before treating SH-SY5Y cells with 10 μM AKNS-2. The results suggested 10 μM AKNS-2 significantly increased LC3-II expression (as shown in Fig. 2B), however this enhancement was significantly inhibited by 3-MA; p62 also plays critical role in autophagy, it binds to LC3 through a region called the LC3-interacting region (LIR) and can be degraded when autophagy is activated (Bjørkøy *et al*., 2009; Moscat and Diaz-Meco, 2009). Interestingly, AKNS-2 also induced a significant reduction in p62 expression (Fig. 2B), and 3-MA treatment markedly blocked the inhibitory effect of AKNS-2 on p62 level. In a tandem fluorescent protein quenching assay, accumulation of GFP-RFP-LC3-II puncta (Fig. 2C) was evaluated using an autophagy sensor from Thermo Fisher Scientific. More cytoplastic puncta stained by green fluorescence and red fluorescence were observed in the transfected cells treated with only AKNS-2 than in the control cells. To confirm that AKNS-2 enhanced autophagy, transfected cells were cotreated with AKNS-2 and the autophagy inhibitors wortmannin (Wort; 50 nM) or bafilomycin A_1 (Baf; 100 nM). As a the PI3K inhibitor, wortmannin inhibits autophagy through blocking the formation of autophagosome (Wu *et al*., 2010), while bafilomycin A_1 prevents lysosomal acidification, thus interfering with the degradation of autophagosome (Yang *et al*., 2013; Yoshii and Mizushima, 2017). AKNS-2-enhanced accumulation of green and red LC3-II puncta was reduced by Wort, while Baf increased green fluorescence and decreased red fluorescence. These findings demonstrated that AKNS-2 activated autophagy.

AKNS-2 protects SH-SY5Y cells against MPP^+-induced neurotoxicity by activating autophagy

We tried to investigate the protective effects of AKNS-2 on an MPP^+-induced *in vitro* PD model. Fig. 3A shows that AKNS-2 did not significantly affect cytotoxicity up to the high concentration of 40 μM by MTT assay. The working concentrations of MPP^+ and AKNS-2 were also determined by an MTT assay. Fig. 3B shows that SH-SY5Y cells were treated with MPP^+ at various concentrations, and MPP^+ at 2 mM significantly re-

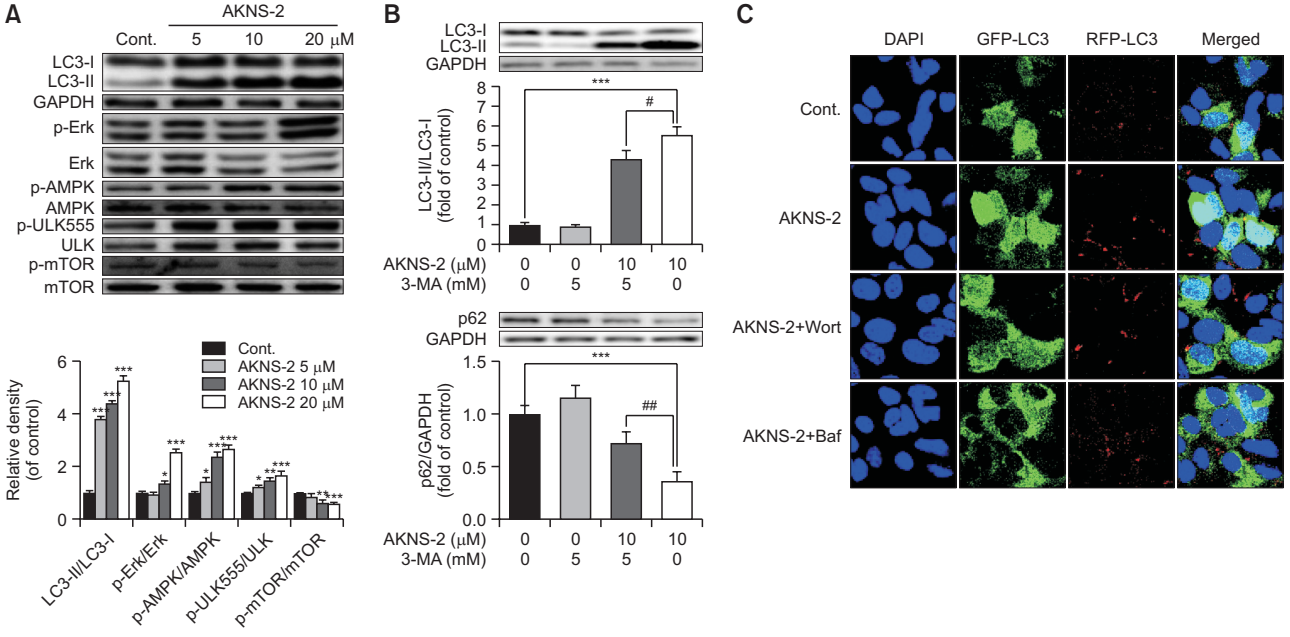

Fig. 2. AKNS-2 activated autophagy through mTOR dependent signals pathway. Twenty-four h after treatment with AKNS-2, key markers involved in autophagy induction in SH-SY5Y cells were measured by Western blot method. (A) shows the expressions of autophagy related protein markers in SH-SY5Y cells treated with AKNS-2. (B) shows AKNS-2 up-regulated LC3-II and reduced p62 expressions were reversed by 3-MA (5 mM). (C) mRFP-GFP-LC3 Tandem Fluorescent Protein Quenching Assay indicates AKNS-2 induced autophagy was inhibited by wortmannin (Wort, 50 nM) and bafilomycin A_1 (Baf, 100 nM). The data are expressed as mean ± SEM (n=3). *p<0.05, **p<0.01, ***p<0.001 significant difference from control, $^{\#}p$<0.05, $^{\#\#}p$<0.01 significant difference from AKNS-2 treated group.

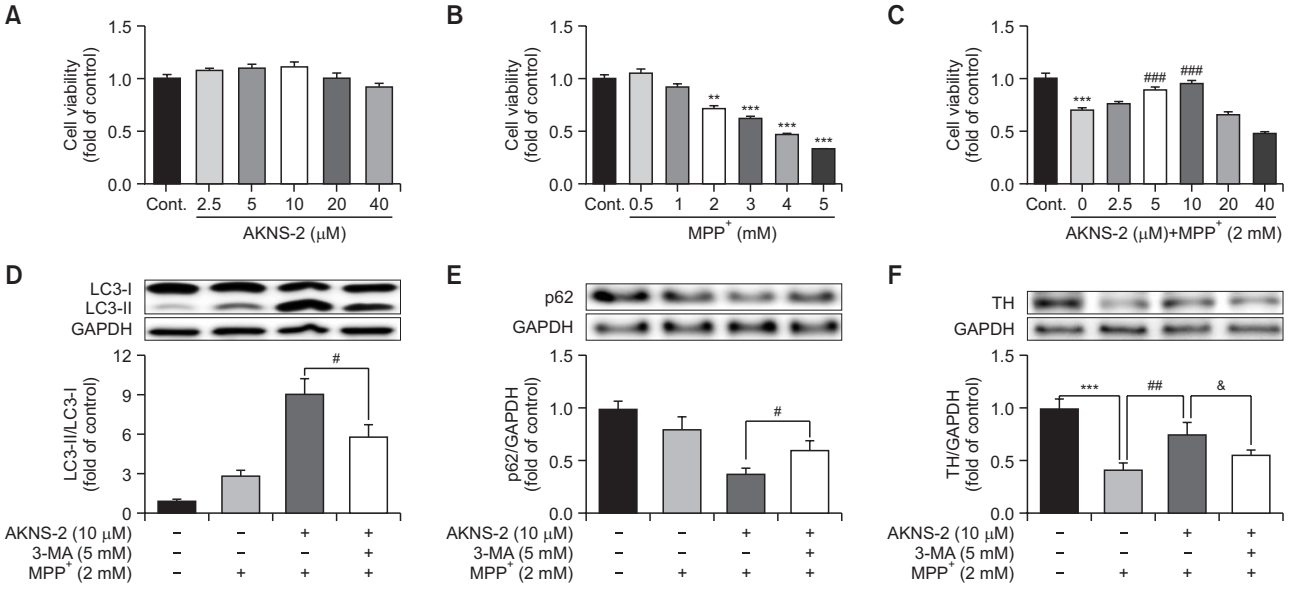

Fig. 3. Protective effect of AKNS-2 on SH-SY5Y cells from MPP^+-induced toxicity was inhibited by autophagy inhibitor 3-MA. (A), (B), (C) show the cell viabilities of SH-SY5Y cells after treatment with AKNS-2 only, MPP^+ only, AKNS-2 and MPP^+ together, respectively, at various concentrations. (D), (E), (F) show the protein expressions of LC3, p62, TH respectively, in SH-SY5Y cells treated with AKNS-2 and MPP^+ in the absence or presence of 3-MA. The data are expressed as mean ± SEM (n=5 for MTT assay, and n=3 for western blot analysis). $^{**}p<0.01$, $^{***}p<0.001$ significant difference from control, $^{\#}p<0.05$, $^{\#\#}p<0.01$, $^{\#\#\#}p<0.001$ significant difference from MPP^+ treated group. $^{\&}p<0.05$ significant difference from AKNS-2 and MPP^+ group.

duced cell viability. Therefore, we decided to induce an *in vitro* PD model using 2 mM MPP^+. Next, we tested the protective effect of AKNS-2 against MPP^+ induced neurotoxicity. Briefly, SH-SH5Y cells were treated with AKNS-2 at various concentrations, and after 1 h, 2 mM MPP^+ was added to the cells. Cell viability was detected 24 h after treatment. The results (Fig. 3C) showed that 5 and 10 μM AKNS-2 markedly enhanced the cell viability impaired by 2 mM MPP^+.

To investigate whether AKNS-2 exerted a protective effect on MPP^+-damaged SH-SY5Y cells by activating autophagy. We employed an autophagy inhibitor, 3-MA, to block the autophagy activated by AKNS-2. Compared to the AKNS-2 and MPP^+ cotreated group, the 3-MA-treated group had significantly inhibited LC3-II expression (Fig. 3D), while the p62 (Fig. 3E) decrease caused by MPP^+ and AKNS-2 was restored by 3-MA. Thus, the autophagy activated by AKNS-2 was blocked by 3-MA. The enzyme tyrosine hydroxylase (TH) is expressed throughout the central nervous system. TH converts tyrosine to L-3,4-dihydroxyphenylalanine (L-DOPA), which can be processed into DA. TH is the rate-limiting enzyme of DA synthesis. Interestingly, in addition to inhibiting autophagy, the MPP^+-induced decrease in TH (as Fig. 3F) expression was reversed by AKNS-2 treatment, and the beneficial effect of AKNS-2 was also abolished by 3-MA treatment.

AKNS-2 upregulates autophagy and protects against MPP^+ neurotoxicity in SH-SY5Y cells by activating the Erk/mTOR pathway

A study reported that the depletion of Erk can partially inhibit autophagy and that the activation of Erk inhibits mTORC1 by binding to and activating TSC, thus upregulating autophagy (Wang *et al*., 2009). U0126 is an inhibitor of the kinase MEK1/2; U0126 prevents the activation of Erk1/2 and can be used to investigate the role of Erk in autophagy induction. To elucidate whether AKNS-2 activates autophagy by modulating the Erk/mTOR signal pathway, SH-SY5Y cells were treated with AKNS-2 (5 and 10 μM) in the absence or presence of U0126 (10 μM). Twenty-four h after cultivation, Western blot analysis was employed to evaluate the induction of autophagy and the expression of protein markers involved in the Erk-modulated autophagy pathway. The results are shown in Fig. 4. LC3-II expression was significantly increased by AKNS-2 (5 and 10 μM) treatment compared with the control condition. When 10 μM U0126 was added 30 min before AKNS-2 treatment, a significant reduction in LC3-II expression (Fig. 4A) was found in both the 5 and 10 μM AKNS-2-treated groups, which indicates that AKNS-2-induced autophagy was inhibited by U0126. A significant increased expression in p-Erk (Fig. 4B) was found in both the 5 and 10 μM AKNS-2-treated groups compared with the control group, while the increased expression of p-Erk in 10 μM AKNS-2-treated cells was dramatically abolished by 10 μM U0126 administration. Afterwards, p-mTOR expression (Fig. 4D) was measured. Compared with the control condition, AKNS-2 (10 μM) significantly inhibited p-mTOR expression, and when 10 μM U0126 was administered 30 min before AKNS-2 treatment, the inhibition of p-mTOR expression induced by AKNS-2 (5 and 10 μM) was markedly recovered. AKNS-2 (5 and 10 μM) significantly enhanced p-ULK555 expression, as shown in Fig. 4C, while 10 μM U0126 abolished the enhancing effect of 10 μM AKNS-2 on p-ULK. Here, we concluded that AKNS-2 upregulates autophagy in SH-SY5Y cells by activating the Erk/mTOR pathway.

TH is the rate-limiting enzyme of DA synthesis. α-synuclein is the primary constituent of the LB, which is one of the pathologic features of PD. The present research aimed to study the protective effect of AKNS-2 on MPP^+-induced neurotoxicity in

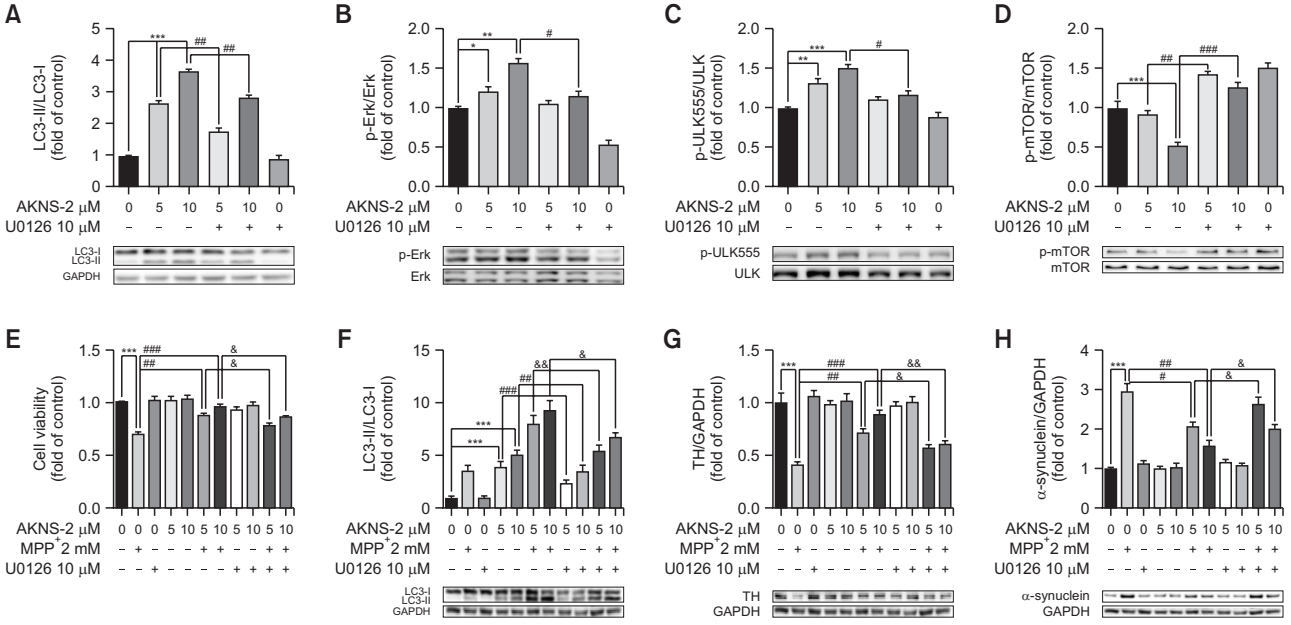

Fig. 4. AKNS-2 exerts its protective effect on SH-SY5Y cells from MPP^+ induced toxicity through activating Erk signal pathway. SH-SY5Y cells were treated with AKNS-2 (5 and 10 μM) in the presence or absence of 10 μM U0126, (A), (B), (C), (D) show the protein expressions of LC3, Erk, ULK, mTOR, respectively. The data are expressed as mean ± SEM (n=3). *p< 0.05, **p<0.01, ***p<0.001 significant difference from control, $^{\#}p$<0.05, $^{\#\#}p$<0.01, $^{\#\#\#}p$<0.001 significant difference from AKNS-2 treated group. SH-SY5Y cells were treated with AKNS-2 and MPP^+ (2 mM) in the presence or absence of 10 μM U0126, (E) shows U0126 abolished the protective effect of AKNS-2 on cell viability; (F), (G), (H) show the expressions of LC3, TH and α-synuclein. The data are expressed as mean ± SEM (n=5 for MTT assay, and n=3 for western blot analysis). ***p<0.001 significant difference from control, $^{\#}p$<0.05, $^{\#\#}p$<0.01, $^{\#\#\#}p$<0.001 significant difference from MPP^+ treated group (for LC3 difference from AKNS-2 treated group). $^{\&}p$<0.05, $^{\&\&}p$<0.01 significant difference from AKNS-2 and MPP^+ treated group.

SH-SY5Y cells. Cell viability was examined by MTT assay. The results in Fig. 4E indicate that AKNS-2 at 5 and 10 μM significantly enhanced the decreased cell viability induced by 2 mM MPP^+, but this enhancement was abolished by U0126 treatment. Next, we examined the expression of LC3 (Fig. 4F). The results showed that U0126 blocked the enhancing effect of AKNS-2 (5 and 10 μM) on LC3-II expression; similarly, the increase in LC3-II expression due to AKNS-2 and MPP^+ co-treatment was also abolished by U0126 administration. These results confirmed that AKNS-2 enhanced cell viability and that AKNS-2 enhanced autophagy and cell viability by modulating Erk signaling. Moreover, TH expression (Fig. 4G) was significantly reduced by 2 mM MPP^+, while the TH reduction could be recovered by AKNS-2 at 5 and 10 μM. When U0126 was administered before AKNS-2 and MPP^+ treatment, the enhancing effect of AKNS-2 on TH expression was inhibited. Regarding α-synuclein expression, 2 mM MPP^+ significantly increased α-synuclein expression (as Fig. 4H) in SH-SY5Y cells, and AKNS-2 treatment counteracted the impact of MPP^+ and inhibited α-synuclein expression. Interestingly, the protective effect was blocked in the presence of U0126. AKNS-2 reversed the altered expression of TH and α-synuclein and enhanced the decreased cell viability by MPP^+ treatment in SH-SY5Y cells; however, these protective effects could be inhibited by disturbing autophagy by blocking the Erk signaling pathway. These facts suggest that AKNS-2 exerts its protective effect on MPP^+ induced cytotoxicity via activating autophagy by regulating Erk signal.

AKNS-2 upregulates autophagy and protects against MPP^+ neurotoxicity in SH-SY5Y cells by activating the AMPK/mTOR pathway

AMPK activation leads to the activation of TSC1/2, thereby inhibiting mTOR activity through inactivating the TOR activator Rheb, which eventually activates ULK1 and autophagy. (Sarkar, 2013). To investigate whether AKNS-2 upregulates autophagy by modulating the AMPK/mTOR pathway, we employed an AMPK siRNA (50 nM) to disturb AMPK signaling in SH-SY5Y cells, and then SH-SY5Y cells were treated with AKNS-2 (5 and 10 μM). Twenty-four h after AKNS-2 treatment, representative protein markers involved in the AMPK/mTOR signaling pathway that modulates autophagy, including LC3, AMPK, mTOR and ULK, were measured by Western blot analysis. Significant increases in LC3-II (Fig. 5A), p-AMPK (Fig. 5B) and p-ULK555 (Fig. 5C) were found in the AKNS-2 treated group compared with the control group. The AKNS-2-enhanced expression of LC3-II, p-AMPK and p-ULK555 was dramatically reduced in AMPK siRNA-transfected SH-SY5Y cells compared with normal AKNS-2-treated SH-SY5Y cells. Additionally, AKNS-2 significantly inhibited p-mTOR expression (Fig. 5D), but the inhibition was abolished in response to disturbance of AMPK signaling.

Next, we tried to elucidate whether AKNS-2 protects SH-SY5Y cells from MPP^+-induced cytotoxicity and to explore the role of AMPK-mediated autophagy in this protection. After SH-SY5Y cells were transfected with 50 nM AMPK siRNA, the cells were treated with AKNS-2 (5 and 10 μM) in the absence or presence of 2 mM MPP^+. Cell viability was test by MTT assay, and as shown in Fig. 5E, significantly decreased cell

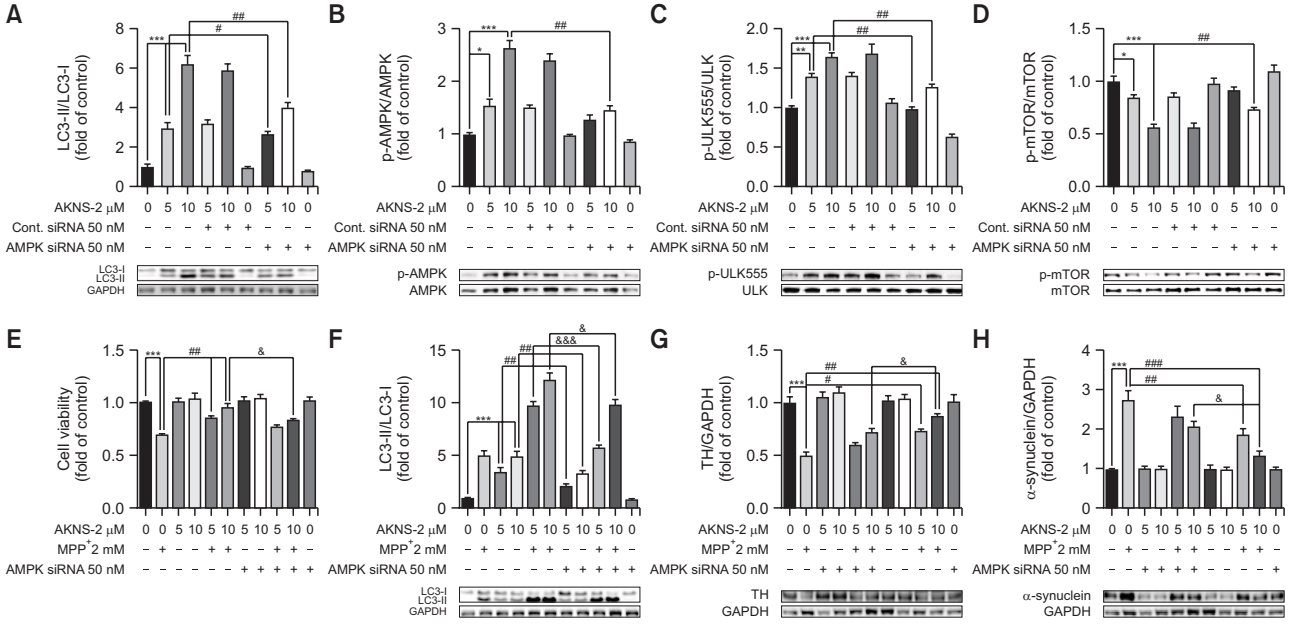

Fig. 5. AKNS-2 exerts its protective effect on SH-SY5Y cells from MPP^+ induced toxicity through activating AMPK signal pathway. SH-SY5Y cells were treated with AKNS-2 (5 and 10 μM) in the presence or absence of AMPK siRNA (50 nM), (A), (B), (C), (D) show the protein expressions of LC3, AMPK, ULK, mTOR, respectively. The data are expressed as mean ± SEM (n=3). *p<0.05, **p<0.01, ***p<0.001 significant difference from control, $^{\#}p$<0.05, $^{\#\#}p$<0.01 significant difference from only AKNS-2 treated group. SH-SY5Y cells were treated with AKNS-2 and MPP^+ (2 mM) in the presence or absence of AMPK siRNA, (E) shows AKNS-2 increased cell viability reduced by MPP^+, AMPK siRNA abolished the protective effect of AKNS-2; (F), (G), (H) show the typical protein bands of LC3, TH, α-synuclein and relative densities. The data are expressed as mean ± SEM (n=5 for MTT assay, and n=3 for western blot analysis). ***p<0.001 significant difference from control, $^{\#}p$<0.05, $^{\#\#}p$<0.01, $^{\#\#\#}p$<0.001 significant difference from MPP^+ treated group (for LC3 difference from AKNS-2 treated group). $^{\&}p$<0.05, $^{\&\&\&}p$<0.001 significant difference from AKNS-2 and MPP^+ treated group.

viability was observed with MPP^+ treatment compared with the control condition, and AKNS-2 (5 and 10 μM) reversed the effect of MPP^+ on cell viability. The viability of AMPK siRNA-transfected SH-SY5Y cells was significantly lower than that of normal SY-SY5Y cells in the presence of ANKS-2 and MPP^+. Regarding the expression of protein markers, LC3-II (Fig. 5F) expression in normal SH-SY5Y cells was markedly enhanced by AKNS-2 (5 and 10 μM), but the LC3-II level in AMPK siRNA-transfected cells was markedly lower than that in normal SH-SY5Y cells in the presence of AKNS-2. Similarly, LC3-II expression was significantly reduced in siRNA-transfected cells after AKNS-2 and MPP^+ cotreatment compared with normal cells. Moreover, TH expression (Fig. 5G) was significantly reduced by MPP^+ administration, and AKNS-2 treatment counteracted the toxicity of MPP^+ and reversed TH expression. Interestingly, the AKNS-2-mediated improvement in TH expression was abolished by AMPK siRNA. MPP^+ significantly increased α-synuclein expression (Fig. 5H), and the increase in α-synuclein level was inhibited by AKNS-2 in normal cells. However, in AMPK siRNA-transfected cells, the inhibition of α-synuclein by AKNS-2 was abolished. These facts indicate that AKNS-2 upregulated autophagy by modulating AMPK signaling and that activated autophagy protects SH-SY5Y cells from MPP^+-induced toxicity.

AKNS-2 improved the behavioral performance of an MPTP-induced in vivo PD model

We also tested the protective effect of AKNS-2 on an MPTP-induced *in vivo* PD model (Fig. 6A showed the scheme). As a non-ergot dopamine agonist, ropinirole delays the motor disorders and is effective in treating early PD (Nashatizadeh *et al*., 2009). In the present study, ropinirole was employed as a positive control to evaluate the protection of AKNS-2 on the induced *in vivo* PD model. First, we tested the effect of AKNS-2 on MPTP-impaired behavioral performance using rotarod test, pole test and wire hanging test. After training, the mice were administered MPTP once daily for 8 consecutive days. The behavioral performance in the rotarod test, pole test and wire hanging test were examined at 2, 24, and 48 h after the last MPTP injection. The mouse behavioral performance in the rotarod test was markedly impaired in the MPTP-treated group compared with the normal group at 2 and 24 h after injection, but the impairment was reversed by 5 mg/kg ropinirole and 15 mg/kg AKNS-2 at 2 and 24 h. Treatment with 5 mg/kg AKNS-2 significantly improved the MPTP-impaired performance in the rotarod test at 24 h. At 48 h, the performance of all mice was recovered to the normal level (as shown in Fig. 6B). MPTP treatment significantly damaged performance in the pole test at 2 h after injection; however, the damaged performance was significantly improved by ropinirole and AKNS-2 administration (5 and 15 mg/kg) at 2 h. No significant differences were found among all groups at 24 and 48 h after MPTP injection (as shown in Fig. 6C). For the wire hanging test, compared with the control condition, MPTP injection significantly decreased the latency to fall at 2 h and 24 h. At 48 h, the MPTP-induced decrease in latency was recovered to the level in pretraining. The positive control ropinirole (5 mg/kg) significantly improved the latency impaired by MPTP at 2 h, while the impaired per-

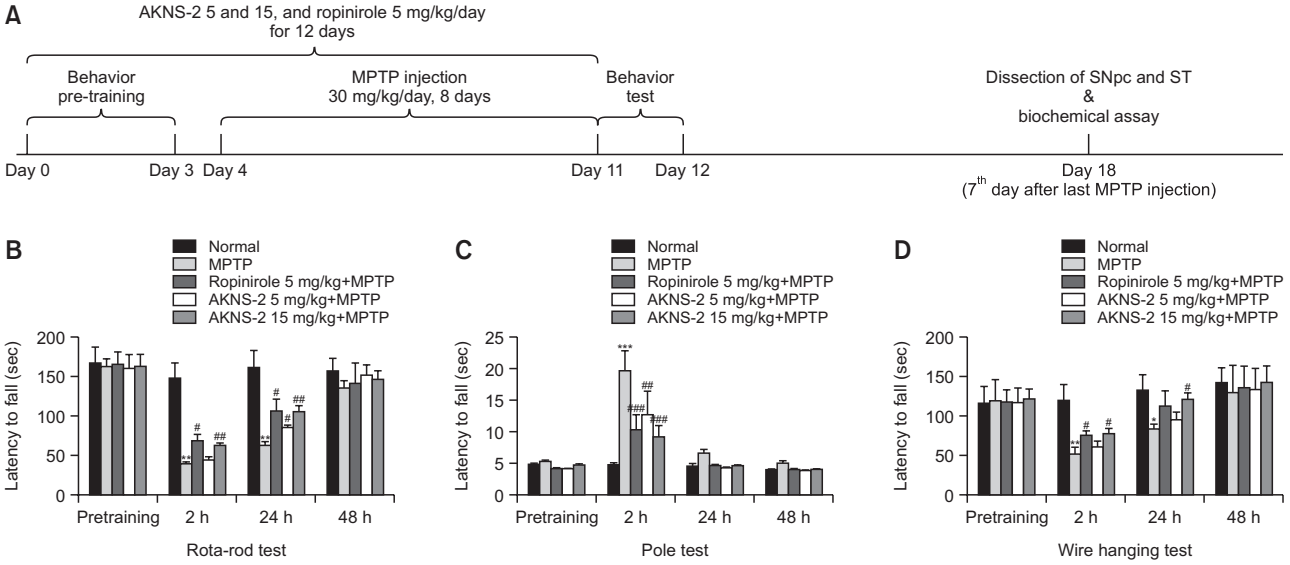

Fig. 6. Protective effect of AKNS-2 on MPTP impaired animal behavioral performance. (A) shows the scheme of sub-chronic MPTP administration-induced *in vivo* PD model. Mice were pre-trained in Rota-rod, Pole and Wire hanging test for 3 days. After the last MPTP injection, mice behavior performances were recorded at different time points. (B), (C) and (D) show the behavior performances of mice in Rota-rod, Pole and Wire hanging test at different time points before or after MPTP administration. The data are expressed as mean ± SEM (n=5). *p<0.05, **p< 0.01, ***p<0.001 significant difference from control group, $^{\#}p$<0.05, $^{\#\#}p$<0.01, $^{\#\#\#}p$<0.001 significant difference from MPTP treated group.

formance in the wire hanging test was significantly improved by 15 mg/kg AKNS-2 at 2 h and 24 h (as shown in Fig. 6D).

Protective effects of AKNS-2 on mice damaged by MPTP administration

DA is a neurotransmitter that transmits signals to other nerve cells in the brain. Dopaminergic neuron damage leads the loss of DA, thereby causing the motor symptoms of PD. The DA level in the ST was measured using an ELISA kit (Abnova). The result (as shown in Fig. 7A) indicated that the DA level in the ST was significantly reduced by 30 mg/kg MPTP administration. Interestingly, the MPTP-induced decrease in DA level was restored by ropinirole (5 mg/kg) and AKNS-2 (15 mg/kg). This result suggested that AKNS-2 protects dopaminergic neurons from the damage induced by MPTP.

MPTP can be converted to MPP^+ by MAO-B in glial cells, and MPP^+ is the actual toxin that damages dopaminergic neurons. MAO-B inhibitors prevent the metabolism of MPTP to MPP^+ by blocking the action of MAO-B. The present research tried to examine whether AKNS-2 protects dopaminergic neurons from the toxicity of MPTP by inhibiting MAO-B activity. MAO-B activities in the SN and ST were detected by a MAO-B assay kit (Promega). The result showed that MPTP (30 mg/kg) significantly enhanced the MAO-B activities in both the ST (Fig. 7B) and SN (Fig. 7C). However, AKNS-2 (5 and 15 mg/kg) failed to reduce the MPTP-enhanced MAO-B activities in both the ST and SN. This fact indicates that AKNS-2 is not an efficient MAO-B inhibitor and that the protective effect of AKNS-2 on MPTP-damaged mice is not due to MAO-B inhibition.

The MPTP-induced PD model is characterized by a decrease in TH in dopaminergic neurons. LBs are one of the pathologic features of PD, and α-synuclein is the primary constituent of LBs. The present research measured the expression of TH and α-synuclein in the ST and SN of MPTP-damaged mice by Western blot analysis. Fig. 7D shows representative immunoblots of TH and α-synuclein in the ST and SN. TH levels were significantly reduced in the MPTP-treated group (30 mg/kg) compared with the normal control group in both the ST (Fig. 7E) and SN (Fig. 7F). Interestingly, the reduction in TH levels in the ST and SN was significantly reversed by the administration of the positive control ropinirole (5 mg/kg) and 5 and 15 mg/kg AKNS-2. As shown in Fig. 7G and 7H, α-synuclein levels were significantly increased by MPTP administration in both the ST and SN, and a significant decrease in the α-synuclein level was observed with the positive control ropinirole at 5 mg/kg compared with MPTP. Moreover, a marked reduction in α-synuclein levels were also found in the ST and SN of AKNS-2-treated (5 and 15 mg/kg) mice compared with MPTP-treated mice.

Autophagy induction by AKNS-2 in an MPTP-induced *in vivo* PD model

AKNS-2 induces autophagy in SH-SY5Y cells, and it protects cells from MPP^+-induced cytotoxicity through autophagy activation. In our MPTP-induced *in vivo* PD model, we tried to examine the effect of AKNS-2 on autophagy regulation. Seven days after treatment with AKNS-2 and MPTP, autophagy-related protein markers in the ST and SN were measured by Western blot analysis. Fig. 8A and 8B show representative immunoblots and the relative intensities of the protein markers in the ST and SN, respectively. The results indicated that MPTP enhanced LC3-II expression to a certain extent, but no significant difference was observed in the ST and ST. Compared with the MPTP treatment, the 15 mg/kg AKNS-2 treatment induced a significant increase in LC3-II expression in the ST. Enhanced LC3-II expression was found in the 15 mg/kg AKNS-2-treated group in the SN, even though no significant difference was ob-

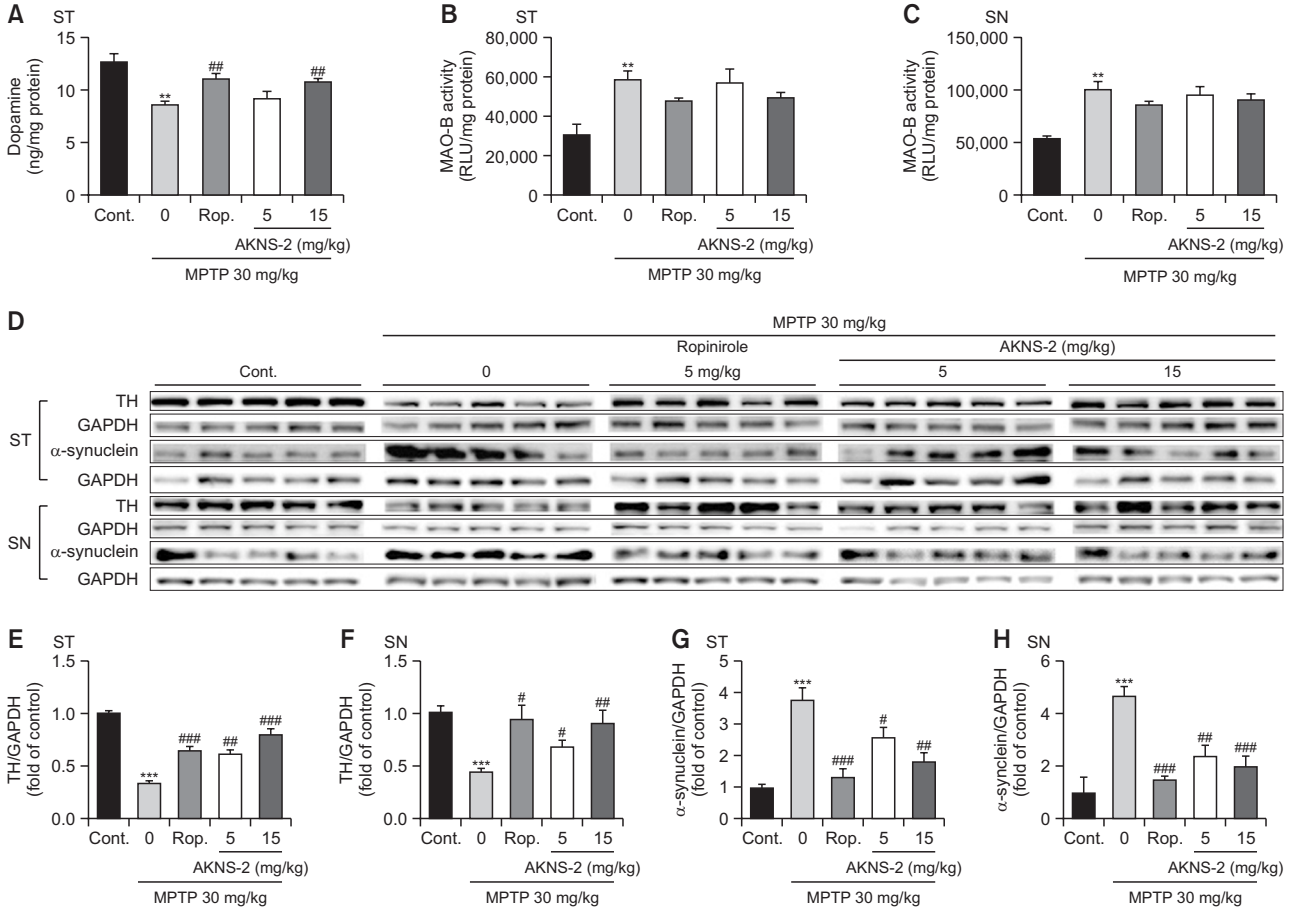

Fig. 7. Protective effect of AKNS-2 on MPTP-induced sub-chronic *in vivo* PD model. Seven days after MPTP injection, mice brain tissues of substantia nigra (SN) and striatum (ST) were dissected for biochemical analysis. (A) shows the dopamine level of ST from each group. (B) and (C) show MAO-B activities of ST and SN, respectively. (D) shows the typical protein bands of TH and α-synuclein in ST and SN, respectively. (E) and (F) show the relative densities of TH from ST and SN, (G) and (H) show the relative densities of α-synuclein from ST and SN, respectively. The data are expressed as mean ± SEM (n=5). **p<0.01, ***p<0.001 significant difference from control group, $^{\#}p$<0.05, $^{\#\#}p$<0.01, $^{\#\#\#}p$<0.001 significant difference from MPTP treated group.

served. Compared with the normal group, the MPTP-treated group showed a significant decrease in p62 expression in the ST, and significantly reduced p62 levels were observed in both the ST and SN in the 5 and 15 mg/kg AKNS-2-treated groups compared with MPTP-treated group. Additionally, MPTP increased p-AMPK expression levels in both the ST and SN. Compared with the MPTP treatment, treatment with ropinirole and AKNS-2 led to significant increases in p-AMPK in both the ST and SN. Moreover, p-Erk expression in the ST and SN was decreased by 30 mg/kg MPTP treatment compared with the control condition and dramatically enhanced by 15 mg/kg AKNS-2 treatment compared with MPTP treatment. Similar to p-Erk expression, p-ULK levels in the ST and SN were markedly reduced by MPTP administration, and the ropinirole and AKNS-2 (5 and 15 mg/kg) treatments counteracted the effect of MPTP and significantly enhanced p-ULK expression in the ST and SN. We also measured p-mTOR expression in mice, and no significant difference was found in the ST or SN between the normal and MPTP-treated groups. Ropinirole and AKNS-2 obviously tended to reduce p-mTOR expression in the ST, even though no significant reduction was observed. In the SN, significant reductions in p-mTOR were found in the ropinirole- and AKNS-2-treated groups.

DISCUSSION

PD is one of the most common neurodegenerative disorders, it is characterized by neuronal cell loss within the SN and formation of LBs due to deficient expression of genes and misfolded α-synuclein (Davie, 2008). Autophagy was reported to efficiently degrade α-synuclein, and the inhibition of autophagy induces the accumulation of insoluble α-synuclein (Vogiatzi *et al*., 2008). Many current PD drugs have failed to prevent the degeneration of dopaminergic neurons (Mythri *et al*., 2012). Natural products, including herbal extracts, phytochemicals and bioactive ingredients, are believed to be potent sources of drugs for PD therapy (Mythri *et al*., 2012). The native Korean plant AKNS is a valuable herb to treat several diseases (Kim *et al*., 2018). The present study aimed to investigate the effect of a triterpene saponin, astersaponin I (named AKNS-2) derived from AKNS on autophagy activation and then to examine

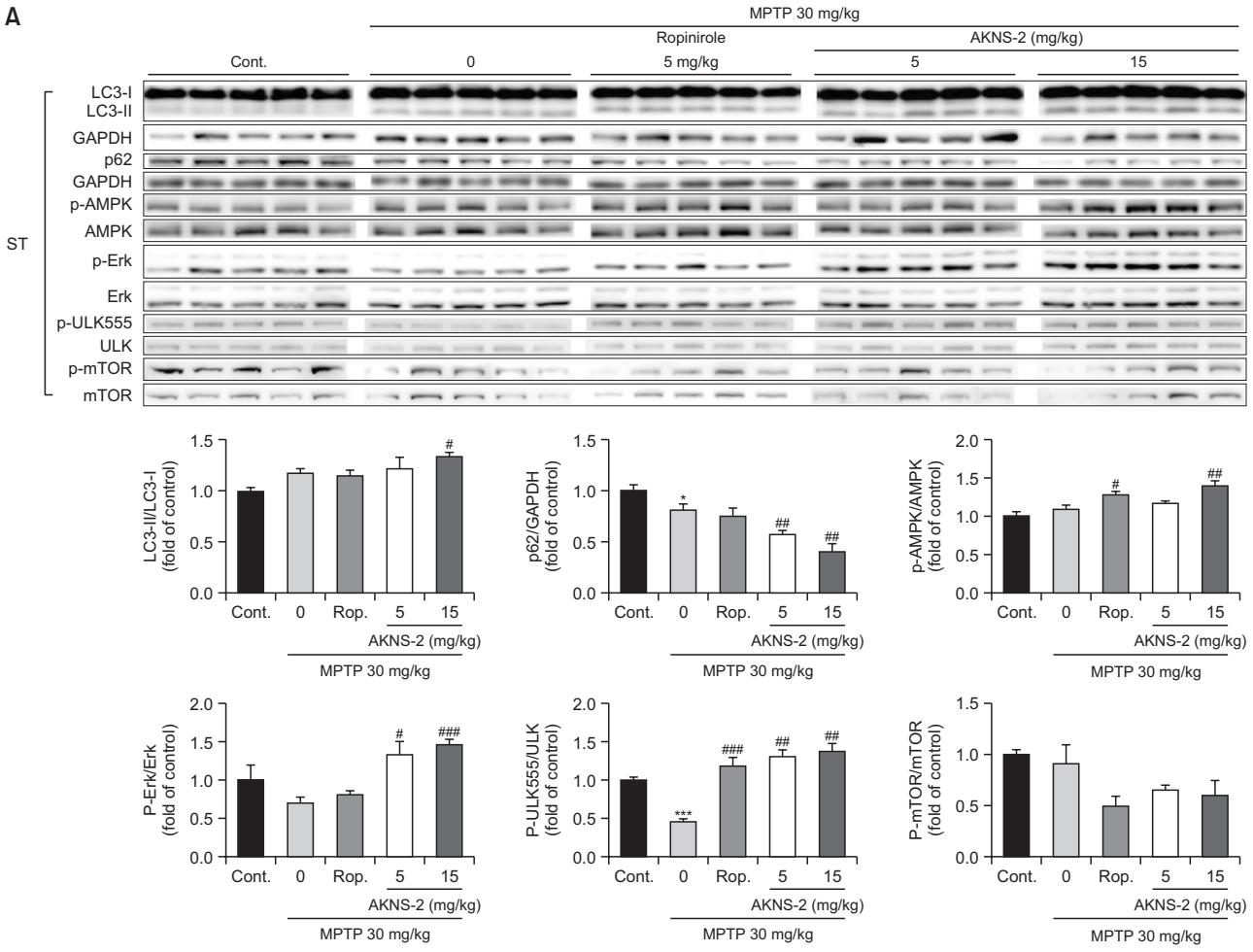

Fig. 8. Autophagy induction of AKNS-2 in *in vivo* experiment. (A) shows the typical protein bands and the relative densities of autophagy related protein markers including LC3, p62, AMPK, Erk, ULK and mTOR in striatum. (B) shows the typical protein bands and the relative densities of autophagy related protein markers including LC3, p62, AMPK, Erk, ULK and mTOR in substantia nigra. The data are expressed as mean ± SEM (n=5). *p<0.05, **p<0.01, ***p<0.001 significant difference from control group, $^{\#}p$<0.05, $^{\#\#}p$<0.01, $^{\#\#\#}p$<0.001 significant difference from MPTP treated group.

its beneficial effect on PD models. The autophagy enhancing effect of AKNS-2 were examined in *in vitro* experiments at various concentrations. The results showed that the AKNS-2 significantly increased the expression of LC3-II, which reflects the amount of autophagosomes and autophagy-related structures (Yoshii and Mizushima, 2017). Next, cytotoxicity was measured by MTT assay in SH-SY5Y cells. AKNS-2 did not show significant cytotoxicity up to 40 μM. To confirm the autophagy-activating effect of AKNS-2, an autophagy inhibitor 3-MA, which inhibits the formation of autophagosomes by blocking class III PI3K, was applied to block autophagic flux (Ito *et al*., 2007). In addition to LC3-II, another important autophagy marker p62, which links LC3 and other ubiquitinated substrates was tested to verify autophagy activation (Zhang *et al*., 2013; Yoshii and Mizushima, 2017). The results revealed that AKNS-2 significantly enhanced LC3-II levels and inhibited p62 levels were dramatically reversed by 3-MA. Furthermore, we also carried out the mRFP-GFP-LC3 tandem fluorescent protein quenching assay to monitor autophagic flux (Zhang *et al*., 2013; Yoshii and Mizushima, 2017). Wortmanin (Wort 50 nM) and Bafilomycin A1 (Baf 100 nM) were employed to inhibit the autophagic flux, respectively. AKNS-2-treatment dramatically increased cellular green and red puncta compared with control group, but the PI3K inhibitor Wort reduced green and red fluorescently labeled LC3 puncta. Moreover, Baf, an autophagy inhibitor which interferes green fluorescence quenching and autophagosome degradation (Zhang *et al*., 2013), produced more green and less red puncta than AKNS-2-treated group. These facts indicated AKNS-2-induced autophagic flux was inhibited, thus, AKNS-2 was confirmed as a potent autophagy inducer.

To explore the underlying pathways that AKNS-2 activates autophagy, we measured other autophagy-related protein markers except LC3-II. We found that AKNS-2 significantly enhance the cellular expression of p-AMPK, p-Erk, p-ULK555, but reduced p-mTOR expression. Supportably, phosphorylated AMPK, Erk upregulate autophagy via inhibiting mTOR, thus enhanced the phosphorylation of ULK (Inoki *et al*., 2003; Meley *et al*., 2006; Ganley *et al*., 2009; Jung *et al*., 2009; Yang *et al*., 2013; Hu *et al*., 2017b). Thus, AKNS-2 may activate au-

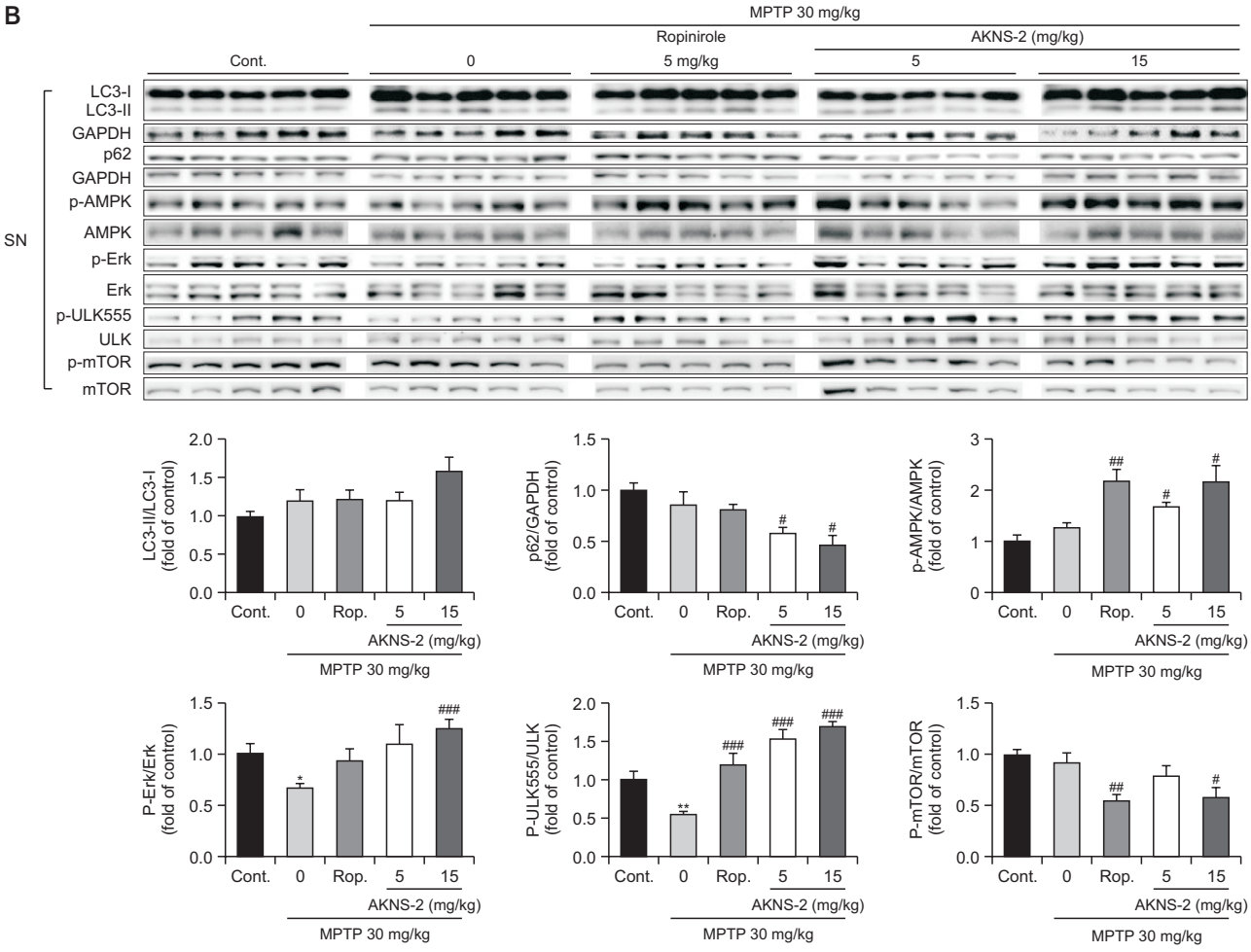

Fig. 8. Continued.

tophagy by modulating the Erk/mTOR and AMPK/mTOR pathways. To clarify the involved autophagy pathways induced by AKNS-2, the Erk inhibitor U0126 was used to block Erk signaling in SH-SY5Y cells. We found that AKNS-2 enhanced p-Erk expression was significantly inhibited by U0126. Moreover, the AKNS-2-induced changes in the expression of downstream autophagy regulators, including p-mTOR and p-ULK555, were reversed by U0126 which subsequently induced a decrease in the ratio of LC3-II/LC3-I. Therefore, AKNS-2 may upregulate autophagy at least partly by modulating the Erk/mTOR pathway. Additionally, the interference of AMPK signaling with siRNA abolished the enhancement of AKNS-2 on p-AMPK, thus reversed the expressions of downstream markers of mTOR, p-ULK555 and LC3-II. These facts suggest that AKNS-2 may also activate autophagy by the AMPK/mTOR pathway.

It is well-known that MPTP, can be converted to the actual neurotoxin, MPP^+, by MAO-B in astrocytes, MPP^+ blocks the mitochondrial respiratory chain and decreases cellular energy, thereby leading to an increase in oxidative stress and cell death (Ransom *et al*., 1987; Janhom and Dharmasaroja, 2015). Thus, MPP^+-induced PD model in SH-SY5Y cells was used to test the neuro-protective effect of AKNS-2. TH, the rate-limiting enzyme in DA synthesis throughout the central nervous system (Tabrez *et al*., 2012; Liang *et al*., 2016), was examined as an index to monitor the protective effect of AKNS-2. The results suggested that TH level was significantly reduced by MPP^+, but AKNS-2 counteracted the effect of MPP^+ and significantly restored the expression of TH. Meanwhile. We found significantly increased LC3-II and deceased p62 expression by AKNS-2 treatment, which indicated the autophagy activation. Interestingly, the changed expressions of TH, LC3-II and p62 were reversed when autophagy was inhibited by 3-MA, which suggested that the protective effect of AKNS-2 was attributed to its autophagy-inducing activity. Furthermore, we tried to examine whether Erk/mTOR and AMPK/mTOR pathways involved in the protective effect of AKNS-2 on the MPP^+-induced *in vitro* PD model. Western blot analysis showed that AKNS-2 and MPP^+ induced changes of LC3-II expression was significantly reversed by Erk inhibitor U0126, which suggested that AKNS-2-induced autophagy was blocked by U0126. Additionally, U0126 abolished the enhancement of cell viability by AKNS-2 in MPP^+ damaged SH-SY5Y cells. Similar results were found when we measured the levels of TH and α-synuclein. AKNS-2 reversed the impaired expression of TH and α-synuclein induced by MPP^+, but U0126 abolished the action of AKNS-2. These results

indicated that AKNS-2 protects against MPP^+-induced neurotoxicity via Erk-activated autophagy. To investigate the involvement of AMPK signaling, AMPK signaling was disturbed by the transfection of AMPK siRNA in SH-SY5Y cells. Results showed AKNS-2 and MPP^+ induced expression change in LC3-II was significantly reversed by AMPK siRNA, which suggested that autophagy was blocked by AMPK siRNA. Meanwhile, AMPK disturbance abolished the AKNS-2 improved cell viability and TH, α-synuclein expressions in MPP^+ damaged SH-SY5Y cells, which suggested a protective effect of AKNS-2 on the MPP^+-induced *in vitro* PD model via AMPK-activated autophagy.

Since *in vitro* experiments demonstrated that AKNS-2 is a potent autophagy inducer and that autophagy activation protects neuronal cells from the toxicity of MPP^+. Next, we tried to test the protective effect of AKNS-2 on an MPTP-induced PD mouse model. The loss of dopaminergic neurons leads to a decrease in DA in the ST, which results in motor disorders, including tremor, rigidity, bradykinesia and postural instability (Taylor *et al*., 2010). After habituation, C57BL/6j mice were subjected to a series of behavioral training regimen (rotarod test, pole test and wire hanging test). Mice behavioral performance were tested at the following three time points: 2 h, 24 h, and 48 h after MPTP (30 mg/kg) injection. Performance in the rotarod test and the wire hanging test was dramatically impaired by MPTP injection, however, 15 mg/kg AKNS-2 significantly improved the impaired performance induced by MPTP in the rotarod and wire hanging tests at 2 and 24 h after MPTP injection. In the pole test, 5 and 15 mg/kg AKNS-2 only alleviated the MPTP-induced behavior impairment at 2 h after the MPTP injection. The behavioral tests in the present research were used to investigate the balance, muscle strength, and motor coordination of animals, and the results reflected the enhancing effect of AKNS-2 on MPTP-impaired mouse behavioral performance.

DA is an important neurotransmitter among of nerve cells in the brain, but it is not sufficiently produced when dopaminergic neurons loss was induced by MPTP, thereby leading to the decrease in DA synthesis and motor disorders found in PD patients (Poewe *et al*., 2017). We measured the DA level in the ST of mice 7 days after MPTP administration. The striatal DA level was significantly reduced by MPTP, and the decrease in DA was restored by 5 mg/kg positive control ropinirole and 15 mg/kg AKNS-2. The enhancing effect of AKNS-2 on the DA level explained the reason why AKNS-2 improved the mouse behavioral performance damaged by MPTP. Moreover, MPTP crosses the BBB and is converted into MPP^+, the actual neurotoxin, by MAO-B in astrocytes (Kupsch *et al*., 2001; Mallajosyula *et al*., 2008). Thus, inhibiting MAO-B activity may also alleviate the toxicity of MPTP and prevent the loss of dopaminergic neurons. The present study tried to clarify whether the protection of AKNS-2 on the MPTP-induced PD model relates to MAO-B activity. The MAO-B activities in the ST and SN were examined by a MAO-B assay kit (Promega), the results did not show any significant difference in MAO-B activity between the MPTP- and AKNS-2-treated groups, which indicated that AKNS-2 was not an efficient MAO-B inhibitor.

We also measured the TH and α-synuclein levels in the ST and SN from mice treated with MPTP and AKNS-2. Consistent with the results of the *in vitro* experiment, MPTP markedly reduced TH levels and enhanced α-synuclein accumulation in both the ST and SN. However, the changes in the expression of TH and α-synuclein induced by MPTP were significantly reversed by AKNS-2, which indicated the protective effect of AKNS-2 against MPTP-induced toxicity. Additionally, we investigated autophagy activation by measuring the expression of LC3-II and p62 in mouse brain using Western blot analysis. The results showed that LC3-II expression in the ST was significantly enhanced by AKNS-2, while the LC3-II level obviously tended to increase in SN. Meanwhile, AKNS-2 significantly decreased p62 levels in ST and SN. Based on these data, autophagy was activated in the *in vivo* PD model. Subsequently, other protein markers related to autophagy regulation were examined, and results were consistent with the *in vitro* experiment, which showed that AKNS-2 significantly upregulated p-AMPK, p-Erk, and p-ULK555 levels and inhibited p-mTOR levels. The upregulated autophagy induced by AKNS-2 is probably due to the activation of the AMPK/mTOR and Erk/mTOR pathways and exerts a protective effect on the MPTP-induced *in vivo* PD model. Autophagy-lysosomal pathway is the one of the major ways for protein degradation in neuron, and it is responsible for the degradation of abnormal aggregated proteins including α-synuclein (Le, 2020). In the present research, AKNS-2 activates the Erk/mTOR and AMPK/mTOR signaling and enhances the transfer of α-synuclein to lysosome by forming the autophagosome, eventually promotes the degradation of α-synuclein and improves the symptoms found in MPTP induced PD models.

The present study reported a novel active compound, AKNS-2, was isolated from natural plant *Aster koraiensis*. We systematically studied the autophagy inducing effect and neuro-protective effect of AKNS-2. Data from the *in vitro* experiments demonstrated that AKNS-2 exerts a prominent autophagy-inducing effect by activating Erk and AMPK signaling, meanwhile, AKNS-2 showed excellent neuro-protective effects on MPP^+ induced *in vitro* and MPTP induced *in vivo* PD model through autophagy activation, it may serve as a candidate for PD therapy.

CONFLICT OF INTEREST

The authors declared no conflict of interest exists.

ACKNOWLEDGMENTS

This work was funded and supported by the Bio-Synergy Research Project (NRF-2012M3A9C4048793) and the Bio & Medical Technology Development Program (NRF-2015M3A9A5030735) of the Ministry of Science, ICT, and Future Planning through the National Research Foundation of the Republic of Korea to HOY. This work also was supported by Korea Institute of Science and Technology (KIST) Institutional Program (2Z05640).

REFERENCES

Bjørkøy, G., Lamark, T., Pankiv, S., Øvervatn, A., Brech, A. and Johansenet, T. (2009) Monitoring autophagic degradation of p62/SQSTM1. *Methods Enzymol.* **452**, 181-197.

Choi, D. Y., Lee, M. K. and Hong, J. T. (2013) Lack of CCR5 modifies glial phenotypes and population of the nigral dopaminergic

neurons, but not MPTP-induced dopaminergic neurodegeneration. *Neurobiol. Dis.* **49**, 159-168.
Chu, Y., Dodiya, H., Aebischer, P., Olanow, C. W. and Kordower, J. H. (2009) Alterations in lysosomal and proteasomal markers in Parkinson's disease: relationship to alpha-synuclein inclusions. *Neurobiol. Dis.* **35**, 385-398.
Conway, K. A., Lee, S. J., Rochet, J. C., Ding, T. T., Harper, J. D., Williamson, R. E. and Lansbury, P. T., Jr. (2000) Accelerated oligomerization by Parkinson's disease linked alpha-synuclein mutants. *Ann. N. Y. Acad. Sci.* **920**, 42-45.
Dauer, W. and Przedborski, S. (2003) Parkinson's disease: mechanisms and models. *Neuron* **39**, 889-909.
Davie, C. A. (2008) A review of Parkinson's disease. *Br. Med. Bull.* **86**, 109-127.
Dehay, B., Bove, J., Rodriguez-Muela, N., Perier, C., Recasens, A., Boya, P. and Vila, M. (2010) Pathogenic lysosomal depletion in Parkinson's disease. *J. Neurosci.* **30**, 12535-12544.
Egan, D. F., Shackelford, D. B., Mihaylova, M. M., Gelino, S. R., Kohnz, R. A., Mair, W., Vasquez, D. S., Joshi, A., Gwinn, D. M., Taylor, R., Asara, J. M., Fitzpatrick, J., Dillin, A., Viollet, B., Kundu, M., Hansen, M. and Shaw, R. J. (2011) Phosphorylation of ULK1 (hATG1) by AMP-activated protein kinase connects energy sensing to mitophagy. *Science* **331**, 456-461.
Ganley, I. G., Lam du, H., Wang, J., Ding, X., Chen, S. and Jiang, X. (2009) ULK1.ATG13.FIP200 complex mediates mTOR signaling and is essential for autophagy. *J. Biol. Chem.* **284**, 12297-12305.
Ghosh, R., Gilda, J. E. and Gomes, A. V. (2014) The necessity of and strategies for improving confidence in the accuracy of western blots. *Expert Rev. Proteomics* **11**, 549-560.
Glick, D., Barth, S. and Macleod, K. F. (2010) Autophagy: cellular and molecular mechanisms. *J. Pathol.* **221**, 3-12.
He, C. and Klionsky, D. J. (2009) Regulation mechanisms and signaling pathways of autophagy. *Annu. Rev. Genet.* **43**, 67-93.
Hu, X., Song, Q., Li, X., Li, D. D., Zhang, Q., Meng, W. H. and Zhao, Q. C. (2017a) Neuroprotective effects of Kukoamine A on neurotoxin-induced Parkinson's model through apoptosis inhibition and autophagy enhancement. *Neuropharmacology* **117**, 352-363.
Hu, X. X., Shi, S., Wang, H., Yu, X., Wang, Q., Jiang, S., Ju, D., Ye, L. and Feng, M. (2017b) Blocking autophagy improves the anti-tumor activity of afatinib in lung adenocarcinoma with activating EGFR mutations *in vitro* and *in vivo*. *Sci. Rep.* **7**, 4559.
Hyun, S.-W., Kim, J., Jo, K., Kim, J. S. and Kim, C. S. (2018) Aster koraiensis extract improves impaired skin wound healing during hyperglycemia. *Integr. Med. Res.* **7**, 351-357.
Inoki, K., Zhu, T. and Guan, K. L. (2003) TSC2 mediates cellular energy response to control cell growth and survival. *Cell* **115**, 577-590.
Ito, S., Koshikawa, N., Mochizuki, S. and Takenaga, K. (2007) 3-Methyladenine suppresses cell migration and invasion of HT1080 fibrosarcoma cells through inhibiting phosphoinositide 3-kinases independently of autophagy inhibition. *Int. J. Oncol.* **31**, 261-268.
Janhom, P. and Dharmasaroja, P. (2015) Neuroprotective effects of alpha-mangostin on MPP(+)-induced apoptotic cell death in neuroblastoma SH-SY5Y cells. *J. Toxicol.* **2015**, 919058.
Jung, C. H., Jun, C. B., Ro, S. H., Kim, Y. M., Otto, N. M., Cao, J., Kundu, M. and Kim, D. H. (2009) ULK-Atg13-FIP200 complexes mediate mTOR signaling to the autophagy machinery. *Mol. Biol. Cell* **20**, 1992-2003.
Kim, J., Kundu, M., Viollet, B. and Guan, K. L. (2011) AMPK and mTOR regulate autophagy through direct phosphorylation of Ulk1. *Nat. Cell Biol.* **13**, 132-141.
Kim, J., Lee, Y. M., Jung, W., Park, S. B., Kim, C. S. and Kim, J. S. (2018) Aster koraiensis extract and chlorogenic acid inhibit retinal angiogenesis in a mouse model of oxygen-induced retinopathy. *Evid. Based Complement. Alternat. Med.* **2018**, 6402650.
Klaidman, L .K., Adams, J. D., Jr., Leung, A. C., Kim, S. S. and Cadenas, E. (1993) Redox cycling of MPP^+: evidence for a new mechanism involving hydride transfer with xanthine oxidase, aldehyde dehydrogenase, and lipoamide dehydrogenase. *Free Radic. Biol. Med.* **15**, 169-179.
Kostrzewa, R. M. (2014) Handbook of Neurotoxicity. Springer, New York.
Kupsch, A., Sautter, J., Götz, M. E., Breithaupt, W., Schwarz, J., Youdim, M. B., Riederer, P., Gerlach, M. and Oertel, W. H. (2001) Monoamine oxidase-inhibition and MPTP-induced neurotoxicity in the non-human primate: comparison of rasagiline (TVP 1012) with selegiline. *J. Neural Transm. (Vienna)* **108**, 985-1009.
Kwon, J., Ko, K., Zhang, L., Zhao, D., Yang, H. O. and Kwon, H. C. (2019) An autophagy inducing triterpene saponin derived from Aster koraiensis. *Molecules* **24**, 4489.
Liang, J. Q., Wang, L., He, J. C. and Hua, X. (2016) Verbascoside promotes the regeneration of tyrosine hydroxylase-immunoreactive neurons in the substantia nigra. *Neural Regen. Res.* **11**, 101-106.
Le, W. (2020) Autophagy: Biologyand Disease- Clinical Science. Springer, Singapore.
Mallajosyula, J. K., Kaur, D., Chinta, S. J., Rajagopalan, S., Rane, A., Nicholls, D. G., Di Monte, D. A., Macarthur, H. and Andersen, J. K. (2008) MAO-B elevation in mouse brain astrocytes results in Parkinson's pathology. *PLoS ONE* **3**, e1616.
Meley, D., Bauvy, C., Houben-Weerts, J. H. P. M., Dubbelhuis, P. F., Helmond, M. T. J., Codogno, P. and Meijer, A. J. (2006) AMP-activated protein kinase and the regulation of autophagic proteolysis. *J. Biol. Chem.* **281**, 34870-34879.
Moscat, J. and Diaz-Meco, M. T. (2009) p62 at the crossroads of autophagy, apoptosis, and cancer. *Cell* **137**, 1001-1004.
Mythri, R. B., Harish, G. and Bharath, M. M. (2012) Therapeutic potential of natural products in Parkinson's disease. *Recent Pat. Endocr. Metab. Immune Drug Discov.* **6**, 181-200.
Nashatizadeh, M. M., Lyons, K. E. and Pahwa, R. (2009) A review of ropinirole prolonged release in Parkinson's disease. *Clin. Interv. Aging* **4**, 179-186.
Noda, T. and Ohsumi, Y. (1998) Tor, a phosphatidylinositol kinase homologue, controls autophagy in yeast. *J. Biol. Chem.* **273**, 3963-3966.
Pattingre, S., Bauvy, C. and Codogno, P. (2003) Amino acids interfere with the ERK1/2-dependent control of macroautophagy by controlling the activation of Raf-1 in human colon cancer HT-29 cells. *J. Biol. Chem.* **278**, 16667-16674.
Poewe, W., Seppi, K., Tanner, C. M., Halliday, G. M., Brundin, P., Volkmann, J., Schrag, A. E. and Lang, A. E. (2017) Parkinson disease. *Nat. Rev. Dis. Primers* **3**, 17013.
Prabakaran, M., Kim, S. H., Mugila, N., Hemapriya, V., Parameswari, K., Chitra, S. and Chunga, I. M. (2017) Aster koraiensis as nontoxic corrosion inhibitor for mild steel in sulfuric acid. *J. Ind. Eng. Chem.* **52**, 235-242.
Ramsay, R. R. and Singer, T. P. (1986) Energy-dependent uptake of N-methyl-4-phenylpyridinium, the neurotoxic metabolite of 1-methyl-4-phenyl-1,2,3,6-tetrahydropyridine, by mitochondria. *J. Biol. Chem.* **261**, 7585-7587.
Ransom, B. R., Kunis, D. M., Irwin, I. and Langston, J. W. (1987) Astrocytes convert the parkinsonism inducing neurotoxin, MPTP, to its active metabolite, MPP^+. *Neurosci. Lett.* **75**, 323-328.
Sarkar, S. (2013) Regulation of autophagy by mTOR-dependent and mTOR-independent pathways: autophagy dysfunction in neurodegenerative diseases and therapeutic application of autophagy enhancers. *Biochem. Soc. Trans.* **41**, 1103-1130.
Tabrez, S., Jabir, N. R., Shakil, S., Greig, N. H., Alam, Q., Abuzenadah, A. M., Damanhouri, G. A. and Kamal, M. A. (2012) A synopsis on the role of tyrosine hydroxylase in Parkinson's disease. *CNS Neurol. Disord. Drug Targets* **11**, 395-409.
Taylor, T. N., Greene, J. G. and Miller, G. W. (2010) Behavioral phenotyping of mouse models of Parkinson's disease. *Behav. Brain Res.* **211**, 1-10.
Vogiatzi, T., Xilouri, M., Vekrellis, K. and Stefanis, L. (2008) Wild type alpha-synuclein is degraded by chaperone-mediated autophagy and macroautophagy in neuronal cells. *J. Biol. Chem.* **283**, 23542-23556.
Wang, J., Whiteman, M. W., Lian, H., Wang, G., Singh, A., Huang, D. and Denmark, T. (2009) A non-canonical MEK/ERK signaling pathway regulates autophagy via regulating Beclin 1. *J. Biol. Chem.* **284**, 21412-21424.
Wu, Y. T., Tan, H. L., Shui, G., Bauvy, C., Huang, Q., Wenk, M. R., Ong, C. N., Codogno, P. and Shen, H. M. (2010) Dual role of 3-methyladenine in modulation of autophagy via different temporal patterns of inhibition on class I and III phosphoinositide 3-kinase. *J. Biol.*

Chem. **285**, 10850-10861.
Yang, Y. H., Chen, K., Li, B., Chen, J. W., Zheng, X. F., Wang, Y. R., Jiang, S. D. and Jiang, L. S. (2013) Estradiol inhibits osteoblast apoptosis via promotion of autophagy through the ER-ERK-mTOR pathway. *Apoptosis* **18**, 1363-1375.
Yoshii, S. R. and Mizushima, N. (2017) Monitoring and measuring autophagy. *Int. J. Mol. Sci.* **18**, 1865.
Zhang, X. J., Chen, S., Huang, K. X. and Le, W. (2013) Why should autophagic flux be assessed? *Acta Pharmacol. Sin.* **34**, 595-599.
Zhu, W., Gao, Y., Wan, J., Lan, X., Han, X., Zhu, S., Zang, W., Chen, X., Ziai, W., Hanley, D. F., Russo, S. J., Jorge, R. E. and Wang, J. (2018) Changes in motor function, cognition, and emotion-related behavior after right hemispheric intracerebral hemorrhage in various brain regions of mouse. *Brain Behav. Immun.* **69**, 568-581.